7. A. I. Vesnitskii, L. A. Ostrovskii, V. V. Papko, and V. N. Shabanov, "Parametric pulse generation," Zh. Éksp. Teor. Fiz., Pis'ma Red., 9, No. 5, 274 (1969).
8. D. A. Kabanov and S. M. Nikulin, "Generation of pulses in a transmission line with parametric diodes," Radiotekh. Élektron., 17, No. 8, 1756 (1973).

LOW-INERTIA PYROELECTRIC DETECTORS FOR RECORDING RADIATION OVER THE 40-1100- nm RANGE

Yu. N. Kiselev and V. Z. Krokhin

UDC 535.231.6:537.227+533.6.011.72

Pyroelectric radiation detectors which make use of the abrupt temperature dependence of the spontaneous polarization in ferroelectrics have a comparatively high sensitivity, a broad spectral response, and a low inertia [1, 2]. Pyrodetectors are usually used to record infrared radiation.

We consider the operation of a longitudinal-type detector which uses a ferroelectric crystal. The polarization vector P is directed along the x axis perpendicular to the electrodes and the radiation is absorbed by one of the electrodes. The pyroelectric current produced in any element $\Delta x\Delta y\Delta z$ of the crystal is determined by the time rate of change of the polarization $dq/dt = \Delta y\Delta z dP/dt$, and the average current in the crystal is proportional to the change in the average temperature

$$\frac{dq}{dt} = \frac{A}{d}\int_0^d \frac{dP}{dT}\frac{dT}{dt}dx; \quad \frac{dP}{dT} = \gamma; \quad \frac{1}{d}\int_0^d \frac{dT}{dt}dx = \frac{d\bar{T}}{dt}; \quad \frac{dq}{dt} = A\gamma\frac{d\bar{T}}{dt},$$

where A is the area of the crystal surface on which the radiation is incident, d is the thickness of the crystal in the direction of propagation of the thermal wave, and $\gamma = dP/dt$ is the pyroelectric coefficient – a constant over some temperature range below the Curie temperature.

If we neglect thermal losses in the crystal, we can write the thermal balance equation in the form

$$cd\,d\bar{T}/dt = ad E/dt,$$

where c is the thermal capacity of unit volume of the crystal, E is the radiation energy density, and a is the radiation absorption coefficient of the crystal.

The measuring circuit can be represented as a current generator connected in parallel with the self-capacity of the crystal C_+, the crystal resistance R_+, the circuit capacity C_-, and the load resistance R_-. The resistance of the crystal is usually much greater than the load resistance ($R_+ \sim 10^{10}$–10^{12} $\Omega\cdot$ cm) and can be neglected. The voltage across the load resistance in the case $R_-C_1 \gg \tau^0$ ($C_1 = C_- + C_+$) is

$$U = (Aa\gamma/C_1 dc)E. \tag{1}$$

and when $R_-C_1 \ll \tau_*$ it is

$$U = (Aa\gamma R_-/dc)\cdot dE/dt. \tag{2}$$

The quantities τ^0 and τ_* are the maximum and typical minimum durations of a radiation pulse. Relationships (1) and (2) define two important modes of operation for a pyroelectric detector: the measurement of the energy of a pulse ($R_-C_1 \gg \tau^0$) and the measurement of its power ($R_-C_1 \ll \tau_*$).

Moscow. Translated from Zhurnal Prikladnoi Mekhaniki i Tekhnicheskoi Fiziki, No. 4, pp. 151-157, July-August, 1976. Original article submitted June 18, 1975.

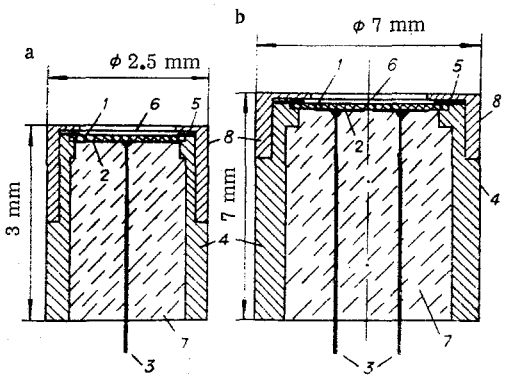

Fig. 1

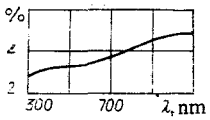

Fig. 2

In longitudinal-type detectors the time resolution is limited by the effect of the upper electrode – the one which absorbs the radiation. The time constant of this type of detector is given by the expression [3]

$$\tau \approx 9c_0^2/kc, \tag{3}$$

where c_0 is the surface thermal capacity of the absorbing electrode and k is the thermal conductivity.

The time resolution of longitudinal-type detectors is usually a few microseconds. There is a somewhat conflicting report in [4] of 30 nsec. The oscillograms shown in the paper indicate a resolving time which is at least 300 nsec.

Radiation detectors used to record strong shock fronts must satisfy rather stringent requirements: they must be able to resolve times of the order of 100 nsec, must have a uniform sesnsitivity over both the visible region and the vacuum ultraviolet, and must be able to record quite strong radiation fluxes. Of some importance under explosive experiment conditions are simplicity of design and a low noise level.

As our sensing element we chose TsTS-19 industrial ceramic which has a pyroelectric coefficient ($\gamma = 5 \cdot 10^{-9}$ c/cm$^2 \cdot$°C) which is constant in the temperature range up to 100°C [2].

Designs were developed for two-section and one-section detectors. With the two-section detector, both the power and energy in the radiation flux can be measured simultaneously. The arrangements are shown in Fig. 1. The TsTS-19 sensing element 1 carries coated electrodes 2 on its lower surface with soldered leads 3. The element is fixed in epoxy resin to the brass body 4 and polished to the required thickness. A layer of silver 5 of the order of 1 μm thickness is applied to the upper part of the body and the edge of the sensing element. A 30-nm layer of gold is then applied to the upper surface to act as the other electrode 6. In Fig. 1, 7 is the epoxy resin and 8 is a brass diaphragm.

A coating of black is applied to the electrode to reduce the reflection coefficient.

It follows from (3) that for a resolving time of 10^{-7} sec with the TsTS-19 detector (c = 3.2 J/cm$^3 \cdot$°C, k = 0.013 W/cm$\cdot$°C), the surface thermal capacity of the upper electrode with its black coating must be less than $2.2 \cdot 10^{-5}$ J/cm$^2 \cdot$°C. It is possible to get such a low value of thermal capacity with gold black [5, 6], which is normally obtained by vaporization of gold in a nitrogen atmosphere. If the absorbing power of the black is to be uniform, it is essential that the oxygen content should not exceed 0.3%. It was difficult under our conditions to get such high-purity nitrogen and so we used industrially "pure" argon with an impurity content of less than 0.01%. We found the following optimum values for the deposition of gold black from a tungsten vaporizer in an argon atmosphere: argon pressure – 0.5 mm Hg, distance from vaporizer to substrate – 3.5 cm, mass of gold charge – 7 mg, and rate of vaporization – 0.5 mg/sec.

Figure 2 shows experimentally measured values of the diffusive reflection coefficient of TsTS-19 ceramic with a 30-nm layer of gold and gold black deposited under the conditions described above. The measurements

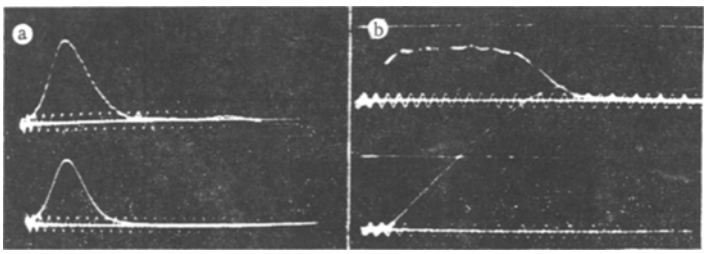

Fig. 3

were made on an SF-4 spectrophotometer with a PDO-1 attachment. It can be seen that the reflection coefficient is less than 5% over the range 300-1100 nm. It is shown in [7] that the reflection coefficient of gold black varies from 2.9% to 1.5% for wavelengths from 220 to 4 nm. In the range 40-120 nm, energy losses occur in photoemission. The sensitivity of the detector in this region can vary by a few percent owing to changes in the photoelectric quantum yield of gold. The maximum losses (5%) occur at $\lambda = 72.5$ nm [7].

The detectors were tested with a 1-μsec radiation pulse from a neodymium laser. The signal from the pyrodetector was fed through a preamplifier (input impedance 75 Ω, gain 100, passband up to 20 MHz) to the input of an OK-33 oscilloscope. The time constant of the electrical circuit was less than 10^{-7} sec.

The second channel of the same oscilloscope displayed for comparison the signal from an FÉK-14 photocell with a resolving time of less than 10^{-8} sec.

Particular attention was paid during the design of the pyrodetectors to the reduction of oscillations associated with piezoresonance of the ceramic element resulting from thermal deformations. The strongest (most slowly decaying) oscillations arose when the sensing element was freely suspended on thin wires. When the ceramic element was fixed in epoxy resin the oscillations decayed much more rapidly. Some reduction in amplitude was observed when the thickness of the element was decreased. Tests were made to see how the oscillation amplitude depended on the size of the lower electrode and the diameter of the diaphragm which limited the radiated surface area. Optimim results were obtained when the diameter of the diaphragm was equal to that of the lower electrode. It can be seen from the oscillograms in Fig. 3a that the detector is able to reproduce satisfactorily the shape of the laser pulse (the upper trace gives the signal from the detector and the lower trace that from the FÉK-14; the period of the sinusoid is 10^{-7} sec). Since the detector must fully reproduce the energy of the pulse, we can estimate the distortion in the shape by drawing the signals from the detector and photocell with amplitude scales chosen so that the areas under the two curves are equal. We can then represent the rise of the detector signal as [1] $\Phi(t) = \Phi_{-}(t)/\sqrt{1 + \tau^2/t^2}$, where $\Phi_{-}(t)$ is the rise in the photocell signal and τ is the time constant of the detector.

The time constant of our detectors has been estimated as not worse than $2 \cdot 10^{-7}$ sec. The maximum measurable pulse length is limited by the time taken for the thermal wave to reach the lower electrode, $t^0 \approx d^2c/4k$.

The sensitivity of the detectors was calibrated by means of a standard ÉV-39 source in which the emitter is a high-current discharge in a capillary tube. The source radiates like a black body at a temperature of 39,000 ± 1000°K. The image of the capillary was focused by a lens onto the detector. The energy density at the detector during the pulse was first measured by an IMO-2 energy recorder. The rms deviation from the average value of energy for a series of 20 measurements with the ÉV-39 source was less than ± 4% for an experimental accuracy of ± 6%. The reproduction of the radiation pulse from the ÉV-39 by the two-section detector is shown in Fig. 3b (upper trace gives the power mode and lower trace the energy mode; period of the sinusoid is 10^{-5} sec). The pulse sensitivity of the energy flux measurements for both designs was as high as 22 W·cm^2/J. This figure agrees with the calculations made for the TsTS-19 material. The sensitivity varied by less than 30% from one detector to another. The various detector parameters are shown in Table 1.

The power range over which the detector has a linear response is determined by the temperature range (below the Curie point) for which the pyroelectric coefficient remains more or less constant. For an infinite half-space whose surface receives a constant thermal flux $a\Phi$ starting at the instant t = 0, the increase in surface temperature is given by

$$\Delta T(0, t) = (2a\Phi/\sqrt{\pi ck})\sqrt{t},$$

i.e., the maximum power flux

$$\Phi^0 = \Delta T\sqrt{\pi ck}/2a\sqrt{t}.$$

TABLE 1

Parameters	One-section detector	Two-section detector
Dectector size	$\phi 2.5 \times 3$ mm	$\phi 7 \times 7$ mm
Size of ceramic element	$\phi 1.8 \times 0.03$ mm	$\phi 5 \times 0.07$ mm
Size of effective absorbing surface	1.7 mm^2	10.6 mm^2
Self-capacity of one section	600 pF	600 pF
Pulse sensitivity for energy	1300 V/J	210 V/J
Pulse sensitivity for power into $R_- = 75\ \Omega$	$4.1 \cdot 10^{-5}$ V/W	$6.6 \cdot 10^{-6}$ V/W
Range of pulse lengths	0.2–500 μsec	0.2–3000 μsec
Spectral range over which the reflection coefficient is less than 6%	40–1100 nm	

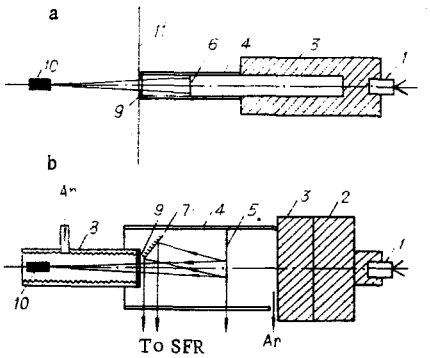

Fig. 4

The sensitivity of the present detectors remained constant right up to values of $\Phi^0 = 20/\sqrt{t}$ W/cm^2, where t is the pulse length in seconds. At higher power fluxes the black started to become transparent as a result of coagulation.

The detectors have been used to measure the radiation from shock fronts in air and argon. A shock wave with a velocity of 13.6 km/sec in air was generated in the 8-mm-diameter cumulation tube of a standard blast source [8] and was released into a glass tube of 8 mm diameter and 10 cm length where it propagated without attenuation (Fig. 4a). The shock wave 5 in this source radiates like a black body with a brightness temperature of 24,000 ± 1000°K right up to the transmission limit of air at 186 nm [8, 9]. Thin black carbon paper 6 was placed at a distance of 5 cm from the end of the glass tube 4 in order to cut off the start of the cumulation where the shock wave is unstable. At the end of the tube there was a steel diaphragm 9 which could cut out the light reflected from the tube walls. Radiation from the explosion products was removed by the opaque screen 11. A one-section detector 10 operating in the power mode was placed along the tube axis (1 is the detonator, 2 is an explosive lens, and 7 is a mirror). Figure 5a shows oscillograms of signals recorded from the detector. The sharp rise in the signal at the end of the trace is due to the expansion of the shock wave as it passes through the diaphragm. The power of the radiation flux incident on the detector through the diaphragm is

$$\Phi = \Phi_+ r^2/(r^2 + b^2),$$

where Φ_+ is the power of the radiation flux from the shock front, r is the radius of the diaphragm, and b is the distance from the diaphragm to the detector.

The radiation flux intensity from the shock front measured in this experiment was $0.82 \cdot 10^6$ W/cm^2 ± 12%; this corresponds to a brightness temperature of 23,700 ± 1200°K and is in good agreement with the spectral measurements [8].

The operation of the detector in the vacuum ultraviolet was tested by measurements of the radiation from a shock front in argon, which transmits radiation right up to 79.8 nm. The shock wave was generated by the emergence of a plane detonation wave onto a charge ring 3 of compressed Hexogen. The wave then propagated

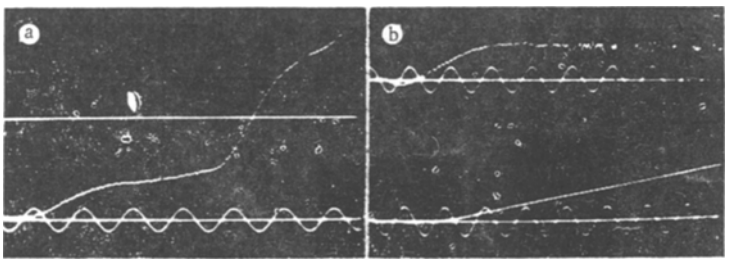

Fig. 5

along a 30-mm-diameter glass tube 4 (Fig. 4b). A two-section detector was placed in a copper tube 8 which had a groove cut in the inside surface. The whole tube was oxidized to a black color in order to eliminate wall reflections. The field of view of the detector was limited by a steel diaphragm. Industrially "pure" argon was blown through the tube during the experiment. One section of the detector operated in the power mode (Fig. 5b, upper trace) and the other in the energy mode (Fig. 5b, lower trace). Simultaneous measurements were also made of the velocity of motion and the brightness temperature of the shock wave in the blue part of the spectrum (430 nm filter with a half-width of 20 nm) by means of an SFR-2M grating photorecorder which had been calibrated with an ÉV-45 standard source. The velocity of the shock wave was constant during the first 6 μsec at 8.8 km/sec ± 5%; the brightness temperature was 24,200 ± 1200°K. The flux intensity measured by the pyrodetector from the shock wave was $1.59 \cdot 10^6$ W/cm^2 ± 12%; this corresponds to a brightness temperature of 23,400 ± 700°K.

Thus measurements of the brightness temperature in the blue part of the spectrum and over the whole spectral range of the shock-wave radiation are in close agreement with each other and correspond to the Hugoniot curve for argon. It should be noted that at a temperature of 24,000°K about half the radiation energy lies in the vacuum ultraviolet. The rise time of the signal from the detector is associated with the rise in the "plug" of the shock-compressed gas. The high accuracy of the brightness temperature measurements in argon made by the detector (3%) is due to the particular dependence of the intensity flux from the shock front in this spectral region, $\Phi_+ \sim T^4$.

The detectors described here could be used to record other processes which produce radiation over a wide spectral range.

The authors would like to express their gratitude to B. D. Khristoforov for a useful discussion.

LITERATURE CITED

1. "Thermal radiation detectors," in: Papers from the First All-Union Symposium [in Russian], Naukova Dumka, Kiev (1967).
2. L. S. Kremenchugskii, Ferroelectric Radiation Detectors [in Russian], Naukova Dumka, Kiev (1971).
3. L. S. Kremenchugskii, "Study of a pyroelectric detector," Opt.-Mekh. Prom-st', No. 10 (1966).
4. A. M. Glass, "Ferroelectric $Sr_{1-x}Ba_xNb_2O_6$ as a fast and sensitive detector of infrared radiation," Appl. Phys. Lett., 13, No. 4 (1968).
5. L. Harris and J. K. Beasley, "The infrared properties of gold smoke deposits," J. Opt. Soc. Amer., 42, 134 (1952).
6. L. S. Kremenchugskii, V. S. Lysenko, A. F. Mal'nev, and O. V. Roitsina, "Determining the thickness, thermal capacity, and thermal conductivity of small thin films," Inzh.-Fiz. Zh., 7, No. 2 (1964).
7. R. G. Johnston and R. P. Madden, "On the use of thermopiles for absolute radiometry in the far ultraviolet," Appl. Opt., 12, No. 4 (1965).
8. E. G. Popov and M. A. Tsikulin, "High-temperature explosive-type emitter for photometry," Zh. Prikl. Mekh. Tekh. Fiz., No. 5 (1970).
9. E. G. Popov, "Radiation properties of shock waves in inert gases and air," Candidate's Dissertation, Moscow Physicotechnical Institute (1969).